International Journal of GEOMATE, Nov., 2025 Vol.29, Issue 135, pp.120-129
ISSN: 2186-2982 (P), 2186-2990 (O), Japan, DOI: https://doi.org/10.21660/2025.135.5157
Geotechnique, Construction Materials and Environment

FLEXURAL BEHAVIOR OF REINFORCED CONCRETE BEAMS RETROFITTED WITH ULTRA HIGH PERFORMANCE CONCRETE USING LOCAL MATERIALS

*Mardiana Oesman[1], Syifa Nadia Iskandar[1] and Muhamad Irfan Nurdin[1]

[1]Department of Civil Engineering, Faculty of Civil Engineering, Bandung States of Polytechnic, Indonesia

*Corresponding Author, Received 26 July 2025, Revised: 06 Sep. 2025, Accepted: 25 Sep. 2025

ABSTRACT: The performance of reinforced concrete (RC) elements often declines over time due to material deterioration, environmental exposure, or changing functional requirements, leading to reduced safety and serviceability. This study investigates the flexural behavior of RC beams retrofitted with Ultra-High-Performance Concrete (UHPC) overlays developed entirely from locally available Indonesian materials, without the use of nanomaterials, making it more practical and sustainable for developing regions. RC beams with a compressive strength of 30 MPa were retrofitted with UHPC layers of 15, 30, 50, and 70 mm thickness, while a 50 mm normal concrete layer served as a control. Experimental testing included load–deflection monitoring, stress–strain measurement, crack pattern observation, and failure mode assessment. Findings revealed that a 30 mm UHPC overlay achieved the highest load-carrying capacity, while 50 mm provided an optimal balance of stiffness, ductility, and toughness. In contrast, 70 mm caused over-reinforcement and brittle failure, and 15 mm offered minimal enhancement. These results demonstrate that UHPC produced from local resources offers an effective, durable, and sustainable retrofitting approach for RC beams in resource-limited settings.

Keywords: Flexural strengthening, UHPC overlay, Sustainable concrete, Retrofitted RC beams, Local materials

1. INTRODUCTION

Reinforced concrete (RC) remains one of the most widely used construction materials globally due to its versatility, cost-effectiveness, and durability under a range of service conditions. Nevertheless, the structural performance of RC elements deteriorates over time as a result of environmental exposure, chemical attack, overloading, aging materials, and changing functional requirements of infrastructure systems. Numerous studies have reported that carbonation, chloride ingress, freeze–thaw cycles, and corrosion of embedded reinforcement are primary contributors to long-term deterioration, often leading to cracking, loss of stiffness, and reduced load-carrying capacity of RC members [1].

For instance, research on bridge decks and marine structures demonstrates that aggressive environmental exposure significantly accelerates corrosion-induced damage, causing service life reduction and increasing maintenance costs [2–5]. As infrastructure in many regions ages, there is growing demand for reliable and sustainable strengthening methods to extend the life of existing assets while minimizing environmental and economic burdens [6,7].

However, UHPC adoption in developing regions is limited by its dependence on costly nanomaterials and imported powders [8]. This study addresses that gap by developing UHPC entirely from locally available Portland Slag Cement (PSC), silica fume, natural sand, and crushed stone (<4.75 mm), eliminating the need for nanomaterials. The research investigates the flexural performance of RC beams retrofitted with UHPC overlays of various thicknesses to demonstrate that sustainable UHPC can provide high structural performance and socio-economic value in resource-limited contexts.

Over the past two decades, various retrofitting approaches have been developed, including fiber-reinforced polymer (FRP) jacketing, steel plate bonding, and overlaying with advanced cementitious composites [9–11]. Although FRP systems offer high strength-to-weight ratios, they present challenges such as debonding, fire vulnerability, and relatively high cost, particularly in developing countries [12]. As an alternative, ultra-high-performance concrete (UHPC) has emerged as a promising material due to its exceptional compressive strength (120–150 MPa), tensile ductility, low permeability, and superior durability [13,14].

UHPC's dense microstructure, optimized particle packing, and steel fiber reinforcement enable superior crack control and resistance to aggressive environments, making it attractive for structural strengthening and rehabilitation [15]. Applications of UHPC have expanded to include bridge deck overlays, seismic retrofitting of columns, and repair of corrosion-damaged elements [16,17]. Recent studies in the *International Journal of GEOMATE* and other leading journals highlight UHPC's potential as a long-term solution for sustainable infrastructure renewal [18,19].

Despite these advantages, UHPC use in developing regions is hindered by reliance on imported, high-cost constituents such as quartz powder, silica flour, and nanomaterials [20]. Consequently, research has focused on developing cost-effective UHPC mixes using locally available materials without compromising mechanical or durability performance [21]. Studies have shown that incorporating supplementary cementitious materials (SCMs), such as ground granulated blast-furnace slag (GGBFS) or fly ash, and regionally sourced aggregates can substantially reduce UHPC production costs while lowering environmental impacts [22]. However, systematic investigations on UHPC overlays for beam strengthening using locally sourced materials are still limited. Moreover, most previous work has emphasized compressive properties and material-level performance, with fewer studies focusing on flexural retrofitting efficiency, optimal overlay thicknesses, and failure mechanisms.

This research addresses these gaps by developing a UHPC mixture entirely composed of locally available Indonesian materials, including Portland Slag Cement (PSC), silica fume, and natural sand, without the use of nanomaterials. The study experimentally evaluates the flexural performance of RC beams strengthened with UHPC overlays of varying thicknesses (15, 30, 50, and 70 mm), compared to a normal concrete (NC) overlay. The investigation encompasses load–deflection behavior, ductility, strain response, crack propagation, and energy absorption characteristics. Unlike many earlier studies, which often emphasize ultra-high compressive strength values, this work focuses on developing a field-practical UHPC with moderate strength (≈68 MPa) that is sustainable, cost-effective, and suitable for tropical field conditions. The findings aim to provide practical design guidance on overlay thickness selection for retrofitting applications and demonstrate how locally sourced UHPC can deliver substantial performance improvements with minimal material use.

The contribution of this study is threefold. First, it demonstrates the feasibility of producing UHPC solely from locally available materials in a developing country context, reducing dependence on costly imported powders and specialized additives. Second, it provides a comprehensive comparison of retrofitting performance across a range of overlay thicknesses, offering quantitative insights into stiffness, ductility, and energy dissipation capacity. Finally, it discusses the potential for UHPC retrofitting to enhance sustainability by extending service life and reducing the need for demolition or reconstruction. Recent literature has emphasized the importance of optimizing retrofit strategies for resource-limited regions, and this study complements that effort by proposing a practical and scalable solution [23].

From a broader perspective, this research contributes to the advancement of sustainable construction materials and methods. It aligns with global initiatives aimed at lowering embodied carbon in cementitious materials by leveraging SCMs, reducing Portland cement content, and promoting circular economy principles [24,25]. In the Indonesian context, where the availability of high-quality imported materials is constrained, developing UHPC formulations that rely on local resources is particularly important for widespread adoption. The insights gained from this study can guide engineers, contractors, and policymakers in selecting efficient strengthening strategies, thereby addressing infrastructure challenges in regions facing budget and material limitations.

The remainder of this paper is organized as follows: Section 2 presents research significance; Section 3 details the materials, mix proportions, specimen preparation, and experimental procedures; Section 4 presents the results and discussion of compressive strength and flexural testing; the structural response in terms of load–deflection behavior, strain profiles, crack patterns, and energy indices; and Section 5 concludes with practical recommendations, sustainability implications, and directions for future research.

2. RESEARCH SIGNIFICANCE

This study introduces a novel approach by developing Ultra-High-Performance Concrete (UHPC) entirely from locally available Indonesian materials, without nanomaterial additives, making it both practical and sustainable for developing regions. Unlike prior research relying on imported or high-cost constituents, this work demonstrates that affordable, locally sourced UHPC can achieve superior mechanical performance in retrofitting applications. The systematic evaluation of varying overlay thicknesses provides new insights into the balance between strength, ductility, and brittleness, offering original design guidance for structural rehabilitation. This research establishes a unique framework for cost-effective, durable, and environmentally conscious strengthening of reinforced concrete structures.

3. MATERIALS AND METHODS

This study experimentally investigated the flexural performance of reinforced concrete (RC) beams retrofitted with ultra-high-performance concrete (UHPC) overlays of different thicknesses. The methodology was designed to ensure reproducibility and to reflect realistic construction practices for field application. All specimens were prepared, cured, and tested in accordance with relevant ASTM standards to enable comparison with previous research and provide credible design guidance.

3.1 Beam Design and Reinforcement Layout

Five simply supported RC beams were fabricated, each measuring 2500 mm in length, 225 mm in depth, and 150 mm in width. The control beam was overlaid with a 50 mm layer of normal concrete (NC), while four beams were strengthened with UHPC overlays of varying thicknesses: 15 mm, 30 mm, 50 mm, and 70 mm. These thickness values were selected to cover practical strengthening scenarios, from minimal overlays to potentially over-reinforced sections. All beams were reinforced with longitudinal D13 steel bars and 6 mm closed stirrups spaced at standard intervals, reflecting typical construction practice in Indonesia

3.2 Concrete Mix Proportions

The NC mix was designed to achieve a target compressive strength of 30 MPa, representing a typical strength class for RC structures. It consisted of Type I Portland cement, natural sand, crushed coarse aggregates (maximum size 25 mm), and water.

UHPC was designed with the Andreasen–Andersen packing model (q = 0.23), using Portland Slag Cement (PSC, ~35–40% slag), silica fume (18,000 m²/kg), fine sand (<2.36 mm), crushed stone (2.36–4.75 mm), water, superplasticizer, and Dramix 3D 80/30 BG steel fibers (aspect ratio 80, length 30 mm) were added to enhance tensile resistance and crack-bridging capacity.

No quartz powder or nanomaterials were used. The mix had a w/b of 0.22, dense packing and a high-range water-reducing admixture (HRWR) to ensure adequate flowability for overlay placement. Workability was evaluated by slump-flow (ASTM C1437), targeting 200–210 mm. The measured average flow was 205 ± 5 mm, indicating adequate self-compacting ability across all overlay thicknesses. Table 1 presents the mix proportions for both NC and UHPC, normalized per cubic meter of concrete.

Table 1. Mix proportions of NC and UHPC

Materials	NC (kg/m^3)	UHPC (kg/m^3)
Type I Portland Cement	457.78	-
Portland Slag Cement	-	750.40
Natural sand	706.38	454.95
Crushed Stone	-	556.05
Coarse aggregate	918.28	-
Silica Fume	-	321.60

Table 2 summarizes the particle size distribution (PSD) of aggregates and supplementary cementitious materials (SCMs).

Table 2. Particle size distribution of aggregates and SCMs

Material	D50 (µm)	Size range (mm)	Notes
Fine sand	250	0.075 – 2.36	River sand, well-graded
Crushed stone	4000	2.36 – 4.75	Angular, locally sourced
PSC	12	<0.045	35–40% slag content
Silica fume	0.15	<0.001	High surface area

This additional PSD table and explicit w/b ratio description provide transparency for reproducibility and clarify the suitability of local materials for UHPC production.

3.3 Specimen Preparation and Overlay Casting

Prior to overlay placement, the surface of each beam was mechanically roughened and cleaned to enhance mechanical interlock between the existing concrete and the new overlay. An epoxy-based bonding agent was applied immediately before casting. The UHPC was mixed in three stages: (1) dry blending of powders and fine aggregates, (2) gradual addition of water and superplasticizer to achieve a slump flow of approximately 205 ± 5 mm (measured per ASTM C1437), and (3) incorporation of steel fibers to ensure uniform distribution.

Overlays were cast in a single pour to minimize cold joints. Specimens were burlap-cured under ambient laboratory conditions (27–31 °C and 65–75% relative humidity), simulating realistic curing in tropical environments. For compressive strength testing, companion UHPC and NC cylinders were water-cured to represent ideal hydration conditions.

3.4 Instrumentation and Test Setup

Flexural tests were conducted using a four-point bending configuration per ASTM C78, with a clear span of 1200 mm. Two hydraulic actuators applied symmetric loading at third points. Vertical deflections were measured using Linear Variable Differential Transformers (LVDTs) placed at midspan and support points. Electrical strain gauges were installed on both longitudinal reinforcement and concrete surfaces to monitor strain distribution and neutral axis shifts during loading.

Figure 1 illustrates the reinforcement details of the test beams, while Figure 2 shows the experimental setup. All load, strain, and displacement data were collected using a digital acquisition system at a frequency sufficient to capture nonlinear structural response.

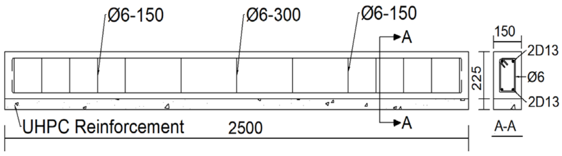

Fig. 1 Reinforced concrete beam diagram

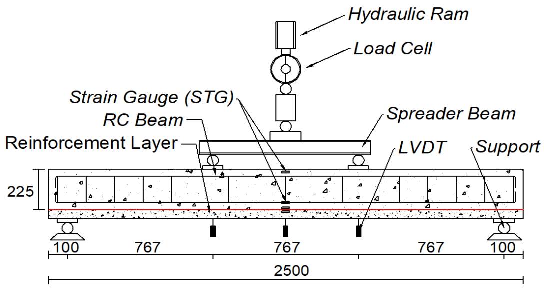

Fig. 2 The experimental setup

3.5 Analytical Parameters

Load–deflection curves were analyzed to evaluate key performance indices, including peak load, initial stiffness, ductility, and energy absorption. Energy-related parameters were calculated as follows:

- Absorption energy (EA): elastic energy stored up to steel yielding,
- Dissipation energy (ED): inelastic energy absorbed from yielding to ultimate load,
- Toughness (ET): total energy absorption (ET = EA + ED). These values were computed numerically using the trapezoidal rule, allowing a detailed comparison of structural performance between specimens. Crack patterns were carefully documented throughout testing to correlate structural response with observed damage mechanisms.

4. RESULTS AND DISCUSSION

4.1 Compressive Strength

In addition to reporting average values, the variability of the material properties has also been considered. Companion compressive strength tests were performed on three cylinders for each UHPC mix, and the mean as well as standard deviation values are reported in Table 3. Compressive strength tests were carried out on cylindrical specimens of both UHPC and normal concrete at 28 and 56 days to evaluate the performance of the proposed local-material UHPC mix.

Table 3. Compressive strength result tests

Samples	28 days (MPa)	Average 28 days (MPa)	56 days (MPa)	Average 56 days (MPa)
UHPC-1	47.71		68.57	
UHPC-2	58.70	53.2	69.74	68.4
UHPC-3	60.27		66.96	
Stdev	6.84		1.40	
NC – 1	24.26	26.0	30.86	30.1
NC – 2	26.12		29.65	
Stdev	1.32		0.86	

At 28 days, the normal concrete (NC) achieved an average compressive strength of 26.0 MPa, while the UHPC mix reached 53.2 MPa—more than double that of NC. At 56 days, UHPC continued to gain strength, reaching 68.4 MPa, whereas NC attained only 30.1 MPa. These findings confirm the effectiveness of the UHPC mixture formulated from local materials in achieving high strength without the use of nanomaterials. Although the compressive strength did not reach the conventional UHPC benchmark of 120–150 MPa, the achieved values were still significantly higher than those of typical structural concrete and sufficient for retrofitting applications. This performance reflects the influence of the local PSC and silica fume grades, which are less reactive compared to imported materials. Nevertheless, the results demonstrate that locally sourced UHPC provides a sustainable and cost-effective option for structural strengthening in developing regions.

Workability tests further confirmed the suitability of the mixture. The slump-flow test yielded an average of 205 ± 5 mm, ensuring uniform placement and consolidation of overlays of varying thicknesses, while minimizing variability in structural response caused by fresh-state behavior.

The compressive strength performance reflects both material composition and curing conditions. Water curing of companion cylinders provided an optimal environment for hydration, resulting in higher compressive strength, while beams cured under burlap in ambient laboratory conditions (27–31 °C, 65–75% RH) exhibited realistic field performance. This distinction highlights the practicality of the proposed UHPC mix for tropical climates, where advanced curing facilities may be unavailable. The dense microstructure achieved through optimized particle packing, combined with the crack-bridging ability of steel fibers, further contributed to the strength enhancement. Previous studies have emphasized the importance of such microstructural optimization, demonstrating that UHPC performance relies not only on cement content but also on particle gradation and binder–fiber interaction [26].

The higher cement content of UHPC undoubtedly contributed to its strength advantage over normal concrete [27]. However, the improvement cannot be attributed solely to cement dosage. Optimized particle packing, the inclusion of silica fume, and the presence of steel fibers collectively enhanced the matrix density and tensile resistance [22,28]. Although a cement-equivalent control mixture was not prepared in this study, the results highlight the holistic benefit of UHPC design rather than binder content alone.

4.2 Load Deflection Curve Analysis

Although only one beam per thickness was tested due to resource constraints, the consistent compressive strength and toughness indices from companion tests support the reliability of the observed trends. Future studies will include additional beam replicates to confirm reproducibility. Because only a single specimen was tested per series, statistical measures such as standard deviations could not be reported, which limits generalization. Nevertheless, the consistent trends observed in peak load, stiffness, energy indices, and crack patterns reinforce the validity of the findings.

Table 4 and Figure 3 compares the structural performance of beams strengthened with different UHPC overlay thicknesses. Beams retrofitted with UHPC demonstrated significantly better flexural behavior than the NC-strengthened beam. The specimen with a 30 mm UHPC layer (B-UHPC 30) achieved the highest peak load (53.78 kN), while the 50 mm UHPC beam (B-UHPC 50) showed a more balanced performance—exhibiting a 14% increase in initial stiffness, an 85% improvement in ductility, and a 33% enhancement in toughness compared to the normal beam (B-Normal 50). These findings indicate that a moderate overlay thickness can effectively mobilize UHPC's superior compressive and tensile strength, leading to substantial gains in load capacity.

The thin overlay of 15 mm (B-UHPC 15) provided minimal improvement, highlighting the limitations of very thin retrofitting layers, while the 70 mm overlay (B-UHPC 70) resulted in an over-reinforced section, reducing energy dissipation efficiency. The balanced performance of the 50 mm overlay demonstrates that there is an optimal thickness range where UHPC's high strength can be fully utilized without compromising ductility. These findings align with studies emphasizing that UHPC's effectiveness is not solely dependent on thickness but also on its ability to achieve composite action with the substrate concrete [33].

Table 4. Load–deflection curve analysis of strengthened beams

Beam Behavior	B-Normal 50	B-UHPC 70	B-UHPC 50	B-UHPC 30	B-UHPC 15
Peak load (kN)	44.64	46.89	50.89	53.78	44.68
Ultimate load (kN)	34.43	42.61	39.08	48.38	33.48
Yield load (kN)	38.15	41.80	45.08	46.85	37.24
Initial Stiffness (EI^{st})	11.89	12.24	13.75	12.52	8.06
Ductility	6.89	9.95	12.74	9.35	5.42
Absorption Energy (kN.mm)	1567.14	849.89	933.616	523.816	423.616
Dissipation Energy (kN.mm)	383.19	1133.17	1653.38	1798.22	907.95
Toughness (kN.mm)	1950.33	1983.06	2586.99	2322.03	1331.57

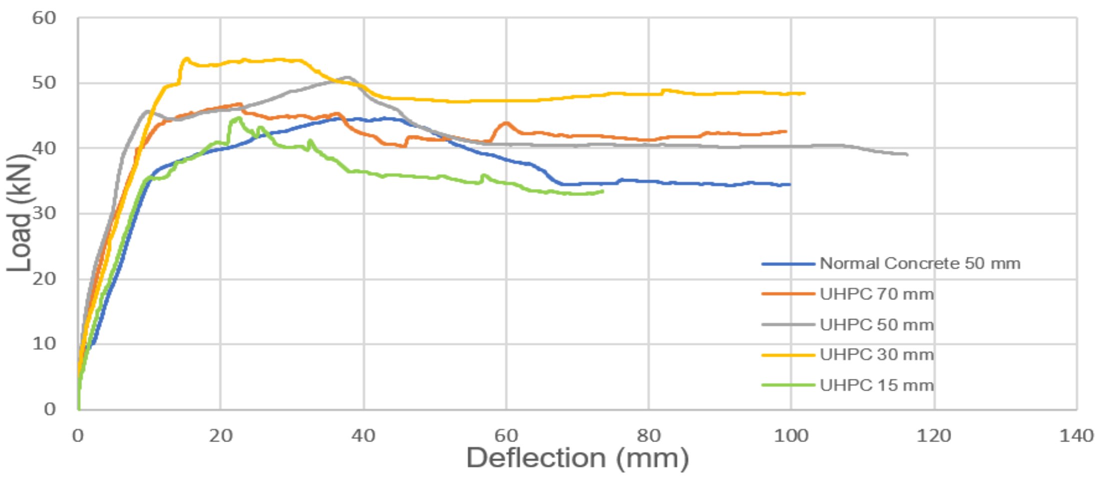

Fig. 3 Load–deflection curves of tested beams under flexural strengthening

The distinction among energy indices clarifies structural response at different service levels. Beams with higher absorption energy demonstrated greater resilience before initial cracking, which implies improved crack-width control at service load levels. Dissipation energy reflects the ability of the beam to sustain deformation and carry load after reinforcement yielding; higher values correlate with residual strength and delayed propagation of flexural-shear cracks. Overall toughness, representing the total energy absorption until failure, provides a combined measure of ductility and structural safety margin.

The results indicate that higher absorption energy corresponds to improved crack control at service levels, while greater dissipation energy reflects superior residual strength beyond yielding. For example, the B-UHPC 50 beam exhibited a toughness of 2587 kN·mm, which was approximately 1.3 times that of the normal concrete control beam. This superior toughness is directly associated with smaller crack widths observed during service loading and improved residual strength after peak load, confirming the practical benefits of UHPC overlays in extending service life.

Figure 3 shows the load–deflection curves for all specimens. B-UHPC 30 had the largest area under the curve, while B-UHPC 50 showed the highest toughness, followed by B-UHPC 30 and B-UHPC 70. Although 50-mm and 70-mm overlays outperformed normal concrete, the 70-mm layer exhibited over-reinforcement, reducing energy dissipation efficiency. The 15-mm overlay provided minimal improvement, confirming that overly thin UHPC layers are ineffective without optimal thickness and bonding.

4.3 Comparative Performance of Overlay Thicknesses

A comparative assessment of overlay thicknesses reveals three key trends. First, increasing overlay thickness beyond 50 mm shifted the neutral axis significantly upward, creating a stiffer but less ductile section, as observed in B-UHPC 70. Second, the 30 mm overlay provided the highest peak strength, confirming that even thin layers of UHPC can deliver significant improvements when properly bonded to the substrate. Third, the 50 mm overlay offered the best balance between strength and deformation capacity, demonstrating its practicality for field applications. These findings corroborate previous research on UHPC overlays for bridge decks, which reported that overlay thickness optimization is critical to achieving both structural efficiency and economic viability [29–31].

4.4 Strain Behavior and Failure Mode

The strain measurements presented in Table 5 illustrate the effect of UHPC overlay thickness on neutral axis depth and failure mechanisms. The control beam (NC 50) and the beam with a 15 mm UHPC overlay exhibited brittle, over-reinforced failure characterized by concrete crushing with negligible reinforcement yielding. Increasing the overlay thickness to 30 mm and 50 mm enabled tensile steel yielding and a more ductile flexural response, confirming effective composite action. The 70 mm overlay beam also reached reinforcement yielding but showed greater stiffness and signs of over-reinforcement, indicating reduced ductility gains at higher thicknesses.

Some calculated neutral axis depths, such as 13.27 mm for B-UHPC 50, appeared unrealistically shallow due to strain concentration and the assumption of a perfectly linear strain distribution, while visual observations indicated deeper neutral axis positions. These discrepancies highlight the limitations of point-gauge measurements, suggesting that future work should utilize Digital Image Correlation (DIC) or denser gauge configurations to obtain more accurate strain-field mapping. Overall, UHPC overlays of 30–50 mm demonstrated superior energy dissipation and improved ductility, while thicker overlays primarily enhanced stiffness without significant ductility gains.

Table 5. Strain behavior and failure mode classification

Sample	Condition	Load (kN)	Strain (mm/mm)				Neutral Line (mm)	Failure mechanism
			STG 1 Concrete	STG 2 Concrete	STG 3 Concrete	STG 1 Steel		
Normal concrete 50	Ultimate	34,43	-0,00206	-0,00018	-0,000002	0,0008	128,93	Over reinfocerd
	Yield	38,15	-0,00141	-0,00006	-0,000004	0,00117	104,60	
UHPC 70	Ultimate	42,61	-0,00212	0,00281	0,000577	0,00563	57,89	Under reinforced
	Yield	41,80	-0,00140	0,00195	0,000605	0,00045	142,27	
UHPC 50	Ultimate	39,08	-0,00004	0,00243	0,000079	0,00213	13,27	Under reinforced
	Yield	45,08	-0,00101	0,00013	0,000012	0,00083	104,13	
UHPC 30	Ultimate	48,38	-0,00294	-0,00003	-0,000012	0,00595	68,72	Under reinforced
	Yield	46,85	-0,00105	0,00002	-0,000006	0,00104	98,80	
UHPC 15	Ultimate	33,48	-0,01906	0,0001	-0,000024	0,00008	175,31	Over reinforced
	Yield	37,24	-0,00102	0,00012	0,000014	0,00061	74,55	

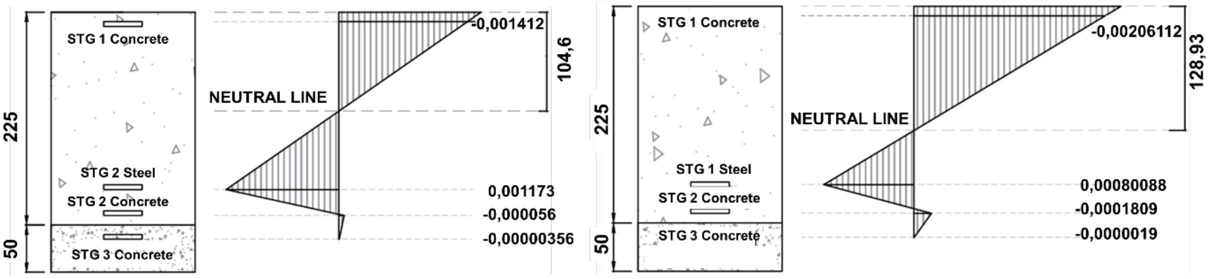

a) At yielding condition

b) At ultimate condition

Fig. 4 Strain diagram of specimen B-UHPC 50

4.5 Crack Pattern Analysis

Crack pattern observations provide further evidence of UHPC's superior tensile performance and bond characteristics The detailed crack patterns for each specimen are illustrated and described in Figures 5-9.

Crack pattern observations provide further evidence of UHPC's superior tensile performance and bond characteristics The specimen strengthened with normal concrete (B-N 50) exhibited early flexural cracks that rapidly propagated, leading to delamination between the overlay and the substrate, which highlighted the poor tensile capacity of normal concrete overlays. . By contrast, beams strengthened with UHPC overlays displayed improved crack control, with cracks distributed more evenly and delayed propagation. The beam with a 15 mm UHPC layer showed crack initiation within the UHPC that extended into the RC substrate; although the bond remained intact, the overall behavior was still brittle and offered limited structural improvement.

Fig. 5 Crack pattern of specimen B-N 50

Fig. 6 Crack pattern of specimen B-UHPC 15

Fig. 7 Crack pattern of specimen B-UHPC 30

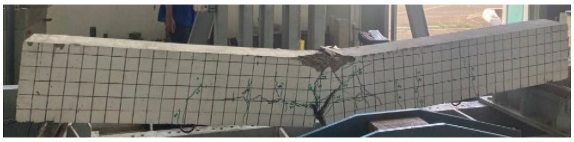

Fig. 8 Crack pattern of specimen B-UHPC 50

Fig. 9 Crack pattern of specimen B-UHPC 70.

The 30 mm UHPC overlay demonstrated a more favorable performance, characterized by dense branching cracks, localized fiber rupture in UHPC, and a strong interface bond, which contributed to a higher load capacity. Similarly, the 50 mm overlay specimen developed extensive flexural-shear cracks while the UHPC layer remained largely crack-free, confirming its high tensile strength and excellent composite behavior. The thickest overlay, 70 mm, showed minimal cracking within the UHPC but experienced brittle crushing in the substrate, suggesting that increased stiffness did not necessarily enhance ductility. Across all retrofitted specimens, no delamination was observed, which validates the surface preparation and bonding procedure. By combining surface roughening and the application of a bonding adhesive, reliable chemical adhesion and mechanical interlock were achieved, ensuring monolithic behavior under flexural loading. These findings align with research indicating that UHPC's dense matrix and steel fiber reinforcement significantly enhance crack resistance and interfacial bond strength [28,32].

4.6 Durability and Sustainability Considerations

Although no direct slant shear or pull-off tests were performed, no signs of debonding or slip lines were observed at maximum load, indicating adequate short-term bond performance. Long-term risks, such as differential shrinkage, creep, and micro-slip under cyclic loading, should be addressed in future research.

In tropical field conditions, the dense UHPC matrix and low water-to-binder ratio (0.22) are expected to minimize moisture ingress and chloride penetration, extending service life. The use of Portland Slag Cement (PSC) and silica fume also reduces clinker content and carbon emissions, making this retrofitting method both environmentally and economically beneficial. Furthermore, replacing a portion of Portland cement with supplementary cementitious materials such as slag significantly reduces clinker demand and embodied carbon emissions, aligning with sustainability goals for low-carbon concrete solutions [25,29].

4.7 Practical Implications

UHPC overlays are well-suited for strengthening bridge decks, industrial floors, and other concrete elements requiring improved flexural capacity and crack control [33]. The 50 mm overlay provides the best balance between strength and ductility, making it a practical choice for field applications. A 30 mm overlay offers a lightweight option when peak load gain is prioritized, while overlays thicker than 70 mm may lead to over-reinforcement and brittle response. By enabling reuse of existing structures, UHPC overlays reduce the need for demolition and new concrete production, lowering life-cycle costs and environmental impact.

4.8 Limitations

This study is limited by the use of a single specimen per overlay thickness, which restricts statistical reliability, and by the absence of direct interface bond tests. Durability assessments under cyclic and environmental loading were also not performed. Despite these constraints, consistent results across strength, stiffness, toughness, and crack pattern observations confirm the validity of the findings. Future studies should include multiple replicates, standardized bond tests, and long-term monitoring to fully validate the performance of UHPC retrofitting systems.

5. CONCLUSION

This study investigated the flexural performance of reinforced concrete (RC) beams retrofitted with ultra-high-performance concrete (UHPC) overlays of varying thicknesses (15, 30, 50, and 70 mm) and compared them with a normal concrete (NC) overlay. The UHPC was designed entirely with locally available materials, including Portland Slag Cement (PSC) and silica fume, without imported powders or nanomaterials, to create a cost-effective and field-practical strengthening solution for developing regions. The following conclusions can be drawn:

- Material performance: The proposed UHPC achieved a compressive strength of 68.4 MPa at 56 days, more than double that of NC (30.1 MPa), demonstrating that a sustainable, locally sourced UHPC mix can deliver high performance without relying on expensive imported materials.
- Flexural behavior improvement: UHPC overlays substantially enhanced beam performance. The 30 mm overlay achieved the highest peak load (53.78 kN), while the 50 mm overlay exhibited the best overall toughness, with a 33% increase compared to the NC control.
- Crack control and interface performance: Crack pattern observations confirmed excellent bond performance, with no signs of delamination or interfacial failure. UHPC's dense matrix and fiber reinforcement contributed to superior crack resistance and energy dissipation.
- Optimal overlay thickness: Overlays thicker than 70 mm increased stiffness but reduced ductility, while very thin overlays (15 mm) offered minimal benefit. A 50 mm UHPC overlay is recommended as a practical and balanced solution for field applications.
- Sustainability implications: The use of PSC and reduced clinker content supports low-carbon construction practices, while retrofitting existing structures minimizes demolition and material waste, extending service life cost-effectively.
- Future research directions: Further studies should include multiple specimen replicates, direct bond strength testing, cyclic loading, and environmental exposure assessments. Advanced strain measurement techniques such as Digital Image Correlation (DIC) are also recommended to improve accuracy in capturing neutral axis depth and crack propagation.

Overall, this research demonstrates that locally produced UHPC overlays can provide a practical, sustainable, and high-performance strengthening technique for RC structures in resource-limited regions, supporting infrastructure resilience and environmental goals.

6. ACKNOWLEDGMENTS

The authors gratefully acknowledge the generous support provided by PT. Bekaert Indonesia for the supply of steel fibers and by PT. Indocement Tunggal Prakarsa Tbk for the provision of Portland Slag Cement. Their contributions were essential to the success of this study.

7. REFERENCES

[1] Chemrouk M. The deteriorations of reinforced concrete and the option of high performances reinforced concrete. Procedia Eng., 2015. https://doi.org/10.1016/j.proeng.2015.11.112

[2] Fuhaid AF Al, Niaz A. Carbonation and Corrosion Problems in Reinforced Concrete Structures. Buildings 2022. https://doi.org/10.3390/buildings12050586.

[3] Dasar A, Hamada H, Sagawa Y, Yamamoto D. Deterioration progress and performance reduction of 40-year-old reinforced concrete beams in natural corrosion environments. Constr Build Mater 2017. https://doi.org/10.1016/j.conbuildmat.2017.05.162.

[4] Awoyera P, Adesina A, Olalusi OB, Viloria A. Reinforced concrete deterioration caused by contaminated construction water: An overview. Eng Fail Anal 2020. https://doi.org/10.1016/j.engfailanal.2020.104715.

[5] Nepal J, Chen HP. Assessment of concrete damage and strength degradation caused by reinforcement corrosion. J. Phys. Conf. Ser., 2015. https://doi.org/10.1088/1742-6596/628/1/012050.

[6] Ghalla M, Bahrami A, Badawi M, Mlybari EA. Novel sustainable techniques for enhancing shear strength of RC beams mitigating construction failure risk. Ain Shams Eng J 2024;15:103017. https://doi.org/https://doi.org/10.1016/j.asej.2024.103017.

[7] Mohammadi-Firouz R, Barros J. Toward Sustainable Strengthening Systems for RC Structures. RILEM Bookseries, 2023. https://doi.org/10.1007/978-3-031-33187-9_92.

[8] Hamad MA, Nasr M, Shubbar A, Al-Khafaji Z, Al Masoodi Z, Al-Hashimi O, et al. Production of ultra-high-performance concrete with low energy consumption and carbon footprint using supplementary cementitious materials instead of silica fume: A review. Energies 2021. https://doi.org/10.3390/en14248291.

[9] Samy K, Fawzy A, Fouda MA. Strengthening of historic reinforced concrete columns using concrete and FRP jacketing techniques. Asian J Civ Eng 2023. https://doi.org/10.1007/s42107-022-00539-4.

[10] Hung CC, Hsiao HJ, Shao Y, Yen CH. A comparative study on the seismic performance of RC beam-column joints retrofitted by ECC, FRP, and concrete jacketing methods. J Build Eng 2023. https://doi.org/10.1016/j.jobe.2022.105691.

[11] Bai Y-L, Zhang Y-F, Sun P-X, Dai J-G, Ozbakkaloglu T. Experimental and Numerical Study on Seismic Performance of PEN FRP-Jacketed Circular RC Columns. J Compos Constr 2023. https://doi.org/10.1061/jccof2.cceng-3983.

[12] Zolfaghari S, Mostofinejad D, Fantuzzi N, Luciano R, Fabbrocino F. Experimental evaluation of FRP-concrete bond using externally-bonded reinforcement on grooves (EBROG) method. Compos Struct 2023. https://doi.org/10.1016/j.compstruct.2023.116693.

[13] Lyu J, Feng S, Zhang Q, Xiao H. Review of factors affecting bond strength between ultra-high-performance concrete and normal strength substrate. Constr Build Mater 2024;439:137416. https://doi.org/https://doi.org/10.1016/j.conbuildmat.2024.137416.

[14] Soni A, Nateriya R. Exploring Ultimate Flexural Strengths of Ultra-High-Performance Concrete (UHPC) Samples through Experimental Analysis in Comparison with Ordinary Concrete Structures. Natl Acad Sci Lett 2024. https://doi.org/10.1007/s40009-024-01520-2.

[15] Gurusideswar S, Shukla A, Jonnalagadda KN, Nanthagopalan P. Tensile strength and failure of ultra-high performance concrete (UHPC) composition over a wide range of strain rates. Constr Build Mater 2020. https://doi.org/10.1016/j.conbuildmat.2020.119642.

[16] Al-Abbas BH, Alsabbagh A, Hasan DM, Semendary AA, Aaleti S. Comparative studies on interfacial bond performance of ultrahigh performance concrete (UHPC) for sustainable repair of bridges and pavements. Results Eng 2024;24:103525. https://doi.org/10.1016/J.RINENG.2024.103525.

[17] Zmetra KM, McMullen KF, Zaghi AE, Wille K. Experimental Study of UHPC Repair for Corrosion-Damaged Steel Girder Ends. J Bridg Eng 2017. https://doi.org/10.1061/(asce)be.1943-5592.0001067.

[18] Tran TH. Cyclic Load-Drift Behavior of Exterior Beam-Column Joints Retrofitted With Ultra-High-Performance Concrete. Int J GEOMATE 2025;28:108–16. https://doi.org/10.21660/2025.128.4925.

[19] Lam NN, Hung L Van. Mechanical And Shrinkage Behavior Of Basalt Fiber Reinforced Ultra-High-Performance Concrete. Int J GEOMATE 2021. https://doi.org/10.21660/2021.78.86151.

[20] Luo Z, Zhi T, Liu X, Yin K, Pan H, Feng H, et al. Effects of different nanomaterials on the early performance of ultra-high performance concrete (UHPC): C–S–H seeds and nano-silica. Cem Concr Compos 2023. https://doi.org/10.1016/j.cemconcomp.2023.105211.

[21] Romero AJ, Moustafa MA. Economic and sustainable UHPC at scale: Material variability study and application to axial columns. J Build Eng 2024;98:111003.

https://doi.org/https://doi.org/10.1016/j.jobe.2024.111003.

[22] Wang D, Zhang Z, Shi C, Wang Y, Ren Q, Ning C, et al. Comparison study of ultra-high performance geopolymer concrete (UHPGC) and ultra-high performance concrete (UHPC): mechanical properties, durability and carbon emissions. Compos Part B Eng 2025;307:112903. https://doi.org/https://doi.org/10.1016/j.compositesb.2025.112903.

[23] Dingqiang F, Yu R, Kangning L, Junhui T, Zhonghe S, Chunfeng W, et al. Optimized design of steel fibres reinforced ultra-high performance concrete (UHPC) composites: Towards to dense structure and efficient fibre application. Constr Build Mater 2021. https://doi.org/10.1016/j.conbuildmat.2020.121698.

[24] Saeed FH, Hejazi F. A Comprehensive Review of Retrofitted Reinforced Concrete Members Utilizing Ultra-High-Performance Fiber-Reinforced Concrete. Materials (Basel) 2025;18. https://doi.org/10.3390/ma18050945.

[25] Miller SA. Supplementary cementitious materials to mitigate greenhouse gas emissions from concrete: can there be too much of a good thing? J Clean Prod 2018. https://doi.org/10.1016/j.jclepro.2018.01.008

[26] Yu J, Cheng Z, Jiang H, Xu X, Liu Y, Gao Y. Influence of the graphene oxide-coated steel fiber on the microstructure optimization of UHPC. Constr Build Mater 2024;452:138921. https://doi.org/https://doi.org/10.1016/j.conbuildmat.2024.138921.

[27] Müller HS, Haist M, Vogel M. Assessment of the sustainability potential of concrete and concrete structures considering their environmental impact, performance and lifetime. Constr Build Mater 2014.https://doi.org/10.1016/j.conbuildmat.2014.01.039.

[28] Parees JA, Gálvez JC, Enfedaque A, Alberti MG. Matrix optimization of ultra high performance concrete for improving strength and durability. Materials (Basel) 2021. https://doi.org/10.3390/ma14226944.

[29] Knigt KA, Cunningham PR, Miller SA. Optimizing supplementary cementitious material replacement to minimize the environmental impacts of concrete. Cem Concr Compos 2023. https://doi.org/10.1016/j.cemconcomp.2023.105049.

[30] Zhang Y, Chai YH. Numerical analysis of bridge deck rehabilitation by ultra-high-performance concrete (UHPC) overlay. Structures 2021. https://doi.org/10.1016/j.istruc.2021.07.044.

[31] Zhou M, Song J, Yin S, Zhu G, Lu W, Lee GC. Cyclic performance of severely earthquake-damaged RC bridge columns repaired using grouted UHPC jacket. Eng Struct 2023. https://doi.org/10.1016/j.engstruct.2023.115615.

[32] Silva ML da, Prado LP, Félix EF, Sousa AMD de, Aquino DP. The Influence of Materials on the Mechanical Properties of Ultra-High-Performance Concrete (UHPC): A Literature Review. Materials (Basel) 2024;17. https://doi.org/10.3390/ma17081801.

[33] Graybeal B, Brühwiler E, Kim B-S, Toutlemonde F, Voo YL, Zaghi A. International Perspective on UHPC in Bridge Engineering. J Bridg Eng 2020. https://doi.org/10.1061/(asce)be.1943-5592.0001630.